STUDYING OPTICALLY ACTIVE COMPONENTS OF THE MIDDLE ATMOSPHERE FROM AN ORBITING STATION

V.V. Butov and S.V. Loginov

Scientific and Production Association "Energiya", Moscow
Design and Technology Institute "Optika", Tomsk
Received October 14, 1995

The method is proposed for reconstruction of the stratospheric ozone concentration, the aerosol extinction coefficient, and aerosol microphysical characteristics from the data on direct solar radiation extinction measured with a spaceborne multichannel spectrometer. Setting the type of aerosol and the altitude profile of its refraction coefficient, we can calculate, for each altitude, the effective function of aerosol particle size distribution g(r, h), as well as to estimate the mean radius of aerosol particles and the width of aerosol particle size distribution function. The technique described was applied to process the experimental data obtained in 1993–1994 by sensing the atmosphere according to the above scheme. Analyzing the contour maps of log(g(r, h)), the vertical profiles of the mean radius, and the widths of the size distribution function, one can obtain the additional information about the stratified structure of the stratospheric aerosol and ozone and separate the regions with several size distribution modes as well as the region of quasihomogeneous aerosol.

Studies of the atmosphere from space by the methods of remote sensing started in early 70s. Instrumentation installed onboard satellites of SBUV, LIMS, SAM, and SAGE types allowed the global monitoring of the distribution of atmospheric constituents in the middle atmosphere. As a rule, this instrumentation had low spatial resolution, therefore it could hardly enable the study of fine structure of the atmospheric constituents distribution. The improved instrumentation was installed onboard satellites of SAGE-II and NOAA types.[1,2] The PSS-1 and PSS-2 devices with specifications similar to SAGE-II were installed onboard the space apparatus SOYUZ-13 and the orbiting station SALYUT-1.[3]

SAGE-II, which continued the set of experiments started by SAM and SAGE, had seven spectral channels in the IR and the visible. The method was developed,[1] which allowed the ozone vertical profile to be reconstructed in the altitude range 10-50 km accurate to 10% and the altitude profile of the aerosol extinction coefficient to be reconstructed in the 10-20 km range with the same accuracy. The discretization step was 1 km. Due to parametrization of the aerosol particle size distribution function, some microphysical characteristics of aerosol were calculated.

The experiment OZAFS (ozone and aerosol fine structure) was performed in 1985 at SALYUT-7 orbiting station.[4] In this experiment, the solar radiation extinction was measured simultaneously with the photographic observations of the twilight earth aureole. The experiment continued studying of the stratified structure of the twilight aureole conducted in 1977-1978 at SALYUT-4 orbiting station. The accuracy of estimating the aerosol extinction coefficient $\beta^a(h)$ and the ozone concentration $N_o(h)$ in the OZAFS experiment was 5-10% with the spatial resolution of 1 km. The device operated in four spectral channels that made it necessary to rigidly set an *a priory* wavelength behavior of the aerosol extinction coefficient. To reconstruct vertical profiles of the ozone and the aerosol extinction coefficient, the reduction method was used that proposed (as in the method of statistical regularization) the use of the covariation matrices of ozone partial pressure and aerosol extinction, therefore it is desirable to conduct the measurements over the regions for which such matrices are already constructed.

Application of multichannel spectrometers, such as SPEKTR-256, GEMMA-2, HRIS, operating in the same wavelength range as SAGE-II allows one (i) to obtain microphysical characteristics of aerosol without parametrization of the aerosol particles size distribution function, (ii) to separate out and calculate more accurately the concentrations of gaseous constituents whose absorption cross sections are in the visible and the near IR. The SPECTR-256 and GEMMA-2 devices have spatial resolution near the horizon of 500 m, whereas HRIS only 150 m. The altitude step is 80 m. Application of multichannel spectrometers provides a possibility of improving reliability and accuracy of studying the fine structure of the distribution of atmospheric constituents.

0235-6880/96/03 219-06 $02.00

When conducting the experiment "Atmosfera-2," we used the technique of occultation sensing, i.e. measured was the direct solar radiation extinction at sunset. The receiver – spectrophotometer was installed onboard the MIR orbiting station (see Fig. 1).

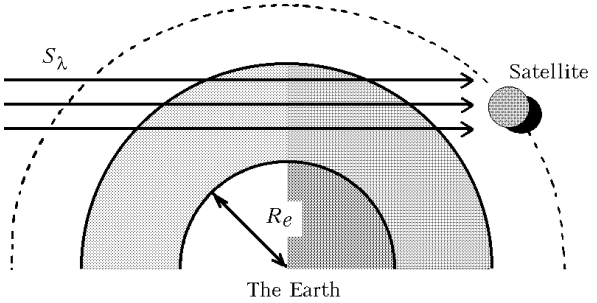

FIG. 1. The experimental geometry. R_e is the Earth's radius.

The experimental geometry and the spectrophotometer specifications provide a possibility to develop a method[6,7] which allows, first, the determination of the vertical distribution of optically active components in the middle atmosphere and, second, the computation of some effective microphysical characteristics of aerosol without the parametrization of the aerosol particle size distribution function. In this work we have changed the algorithm for separating signals used in further calculations. The criteria for sorting were as follows: 1) optical depth computed by the models of standard atmosphere, corresponding to measurement place and time, should be typical, 2) the regression equation describing the wavelength dependence of the logarithm of optical depth should have negative character and be stable. The method is based on the following principles:

1) Since at altitudes above 15 km the value of Rayleigh depth $\tau_\lambda^r(h)$ differs from that corresponding to the standard atmosphere by no more than 3%, the model of standard atmosphere can be used for the determination of the Rayleigh depth. For the spectral range 0.45–0.83 μm, where the device operates, ozone can be considered as absorbing mainly in the 0.55–0.73 μm Chappuis band and the wavelength dependence of the aerosol depth can be described by the Angstrom formula. So, having estimated the aerosol depth $\tau_\lambda^a(h)$ in the 0.45–0.55 and 0.75–0.83 μm ranges and extrapolated it onto the Chappuis band, we can find the ozone depth. Similar procedure was used in Refs. 4 and 5. The procedure used in Refs. 6 and 7 was somewhat different, because $\tau_\lambda^a(h)$ and the power ν were determined there from the measured depth $\tau_\lambda(h)$ values. Errors in determination of $\tau_\lambda^a(h)$ and the power ν as rms deviations were no more than 3 and 5%, respectively.

2) Vertical profiles of the aerosol extinction coefficient $\beta^a(h)$ and the ozone concentration $N_o(h)$ were reconstructed from the depth measured using regularization methods.[8,9] The calculation error did not exceed 5–10%.

3) To find the particle size distribution function we used the method proposed in Ref. 10. Its idea is in the use of the characteristic aerosol scale to linearize the dependence of the aerosol depth on the extinction efficiency factor and the particle size distribution function. We have processed the aerosol optical depths determined in the spectral ranges outside the Chappuis band, i.e. in the 0.45–0.53 and 0.75-0.83 μm ranges. In computations we used the extinction efficiency factor, calculated by Mie theory, for spherical homogeneous particles with the radius r and the complex refractive index m close to unity.[11]

The microphysical parameters of aerosol, such as the mean particle size $\langle r \rangle$ and the width of the particle size distribution δr, were calculated as mean and rms deviations of the distribution $g(r, h) = rf(r, h)$ normalized to the number of aerosol particles having the size within 0.1–3 μm. The calculation errors were 5–25% for $f(r)$ and 25% for $\langle r \rangle$ and δr.

SOME RESULTS OF ATMOSPHERIC SENSING

The solar radiation extinction by the atmosphere was measured with a spectrophotometer having the following performance characteristics: the operating range 0.45–0.83 μm, the number of spectral channels 128/256, and the channel width 3/1.5 nm, respectively. For the device to operate throughout the entire operating range, the combined filter was used, which was assembled from NS11– and ZS8–type glasses. Changes in the Sun brightness S_λ when displacing the sight line (SL) from the disk center to its edge was given by the model from Ref. 12. Since the Sun brightness varies markedly over the disk, the SL position with respect to the center should be taken into account. The SL drift over the disk due to refraction was taken into consideration by the standard refraction model.[13] Movement of the sight line due to permanent movement of the station was found at high Sun from the rate of brightness change in the shortest wavelength range. Having referred the photo data we found the distance between the sight line and the center of the solar disk being at the altitude h = 26–27 km from the degree of deformation of the solar disk image due to refraction. Allowance for the above factors permitted us to reconstruct the sight line drift over the solar disk accurate to < 1′. This corresponds to the error in brightness reconstruction of the order of 5%, that is comparable with the instrumental noise.

The solar disk was spectrometered during the sunset on 16.04.1992 (experiment I), 14.10.1992 (experiment II), 22.01.1993 (experiment III), and 31.05.1994 (experiment IV) from onboard the orbiting station MIR. The perigee of the sight line during the experiments was over points with the following geographical coordinates: 48.08 S, 27.12 W; 50.12 S,

55.12 E; 22.45 S, 12.79 W; 41.41 S, 92.72 W, respectively.

Following the above-described technique for processing the optical depths measured, we obtained the altitude profiles of the aerosol extinction coefficient $\beta^a(h)$ (reference wavelength λ_{ref}=0.79 μm), the ozone concentration $N_o(h)$, the mean radius of aerosol particles $<r(h)>$, and the width of the aerosol particle size distribution $\delta r(h)$ (Figs. 2 and 3). The calculation results were smoothed by a simple moving averaging with the scale corresponding to the spatial resolution of the device, for the geometry used it was 0.5 km. When estimating δr, we used the models of the particle refraction index proposed in Refs. 14–16. The data from Ref. 2 were used to estimate $<r(h)>$ and δr at an altitude of 20 km (Fig. 3*b*). For experiments II–IV presented are the values corresponding to the model aerosol. Figure 3 shows the map, on which isolines and different darkening demonstrate the altitude distribution of aerosol particles with size from 0.1 to 5 μm. For more vivid picture, calculated was the function log ($g(r, h)$) with values reduced to the unit interval at every altitude level. It was constructed on the 30×30 grid. In figure corresponding to experiment I, bars are for errors in reconstruction of vertical profiles.

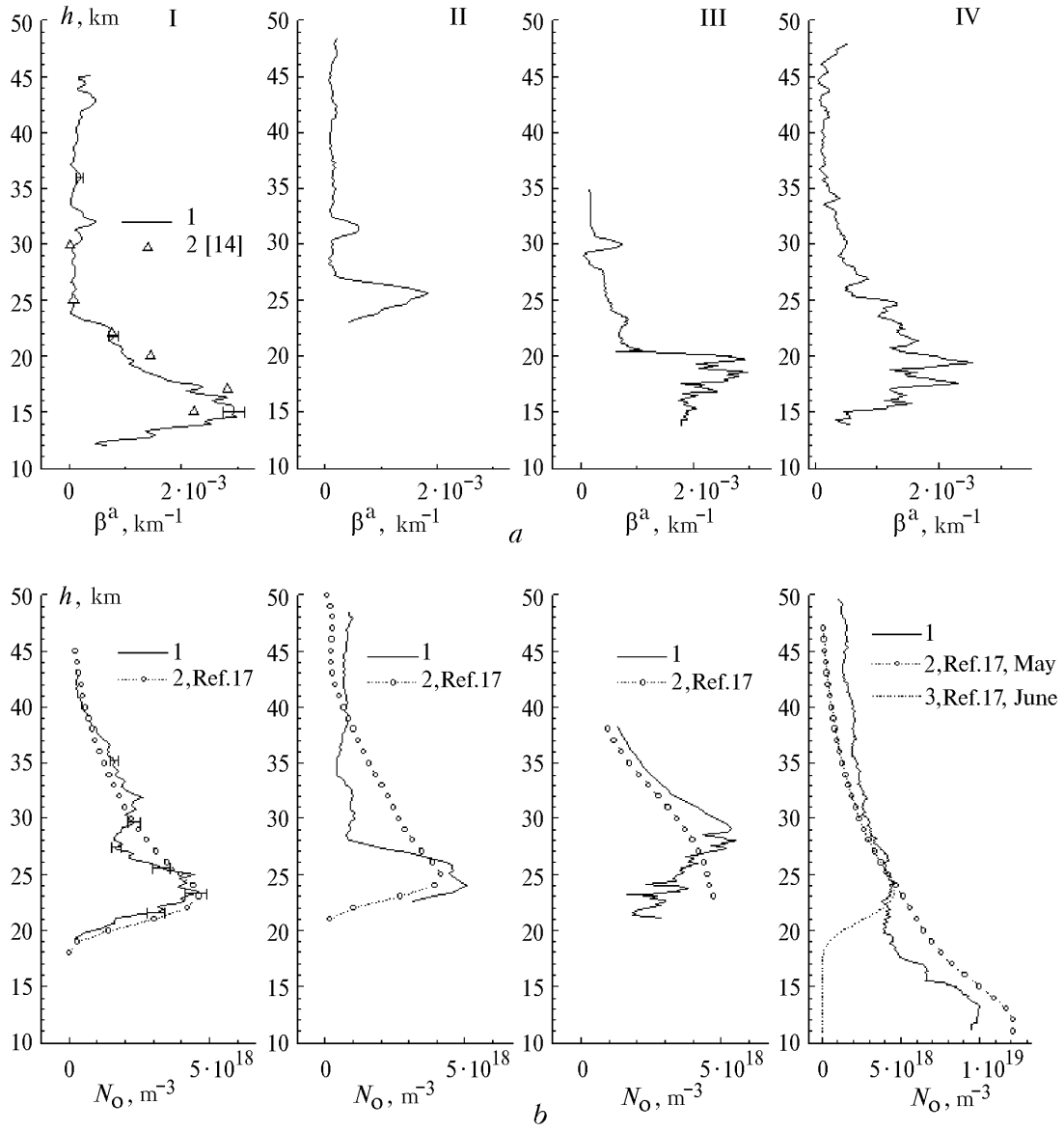

FIG.2. The vertical profiles of the aerosol extinction coefficient (a) and the ozone concentration (b): the reconstructed profiles (1), and the model profiles (2 and 3). The dates of experiments and the coordinates of the point of beam perigee: 04.15.92, 48.08 S, 27.12 W *(experiment I), 10.14.92,* 50.12 S, 55.12 E *(II), 01.22.93,* 22.45 S, 12.79 E *(III), 05.31.94,* 41.41 S, 92.22 E *(IV).*

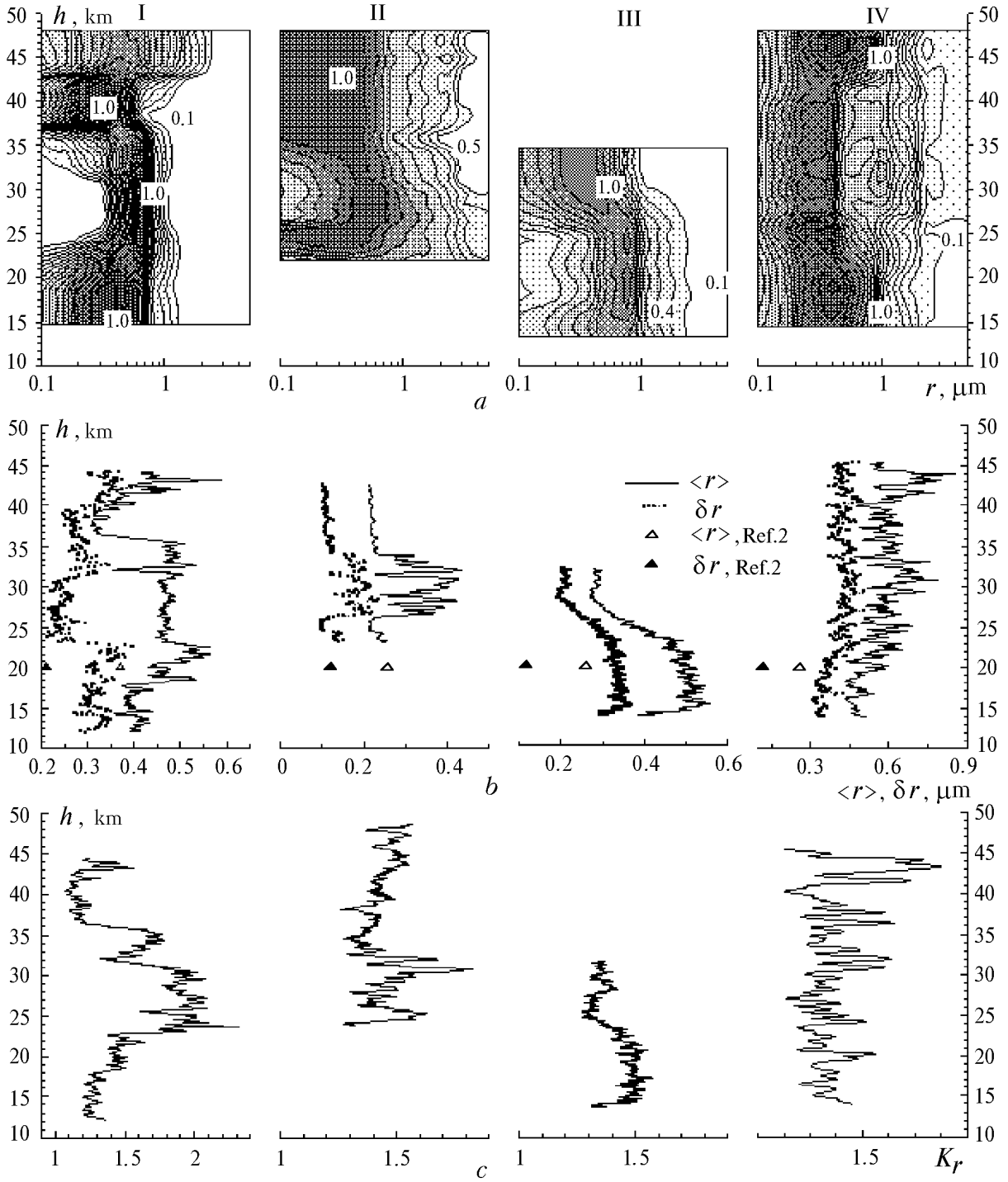

FIG. 3. Some characteristics of the stratospheric aerosol: (a) contour maps of the size distribution of the stratospheric aerosol, (b) vertical profiles of the mean radius of aerosol particles <r(h)> and the width of the aerosol particle size distribution function δr(h), (c) vertical profile of the ratio K_r = <r(h)>/δr(h).

Analysis of the results obtained allows us to reveal the following peculiarities (Figs. 2 and 3):

– The effect of the season and the latitude of the place upon the distribution of ozone and aerosol in the stratosphere, especially, upon the positions of maxima of their concentrations, is clearly seen.

– From the figures corresponding to the measurements conducted in 1992–1993 (experiments I–III), most pronounced are the peculiarities of the aerosol vertical distribution (Fig. 2a). Aerosol layers are seen at the altitude: 14–20 km (Junge layer), 22–23, and 32 km. In experiment I, aerosol making up

these layers has the following characteristics: 14–20 km layer: $\langle r(h)\rangle \sim 0.4$ μm, $\delta r(h) \sim 0.3$ μm; 22.5 and 33 km layers: $\langle r(h)\rangle \sim 0.52$–$0.54$ μm and $\delta r(h) \sim 0.4$ μm (Fig. 3*b*). These layers are formed from particles whose size varies within a wide range (Fig. 3*a*). At the same time, the aerosol extinction coefficient distribution at these altitudes was stratified, it is especially clear with the particles forming the Junge layer. At altitudes 23–34 km there was the aerosol having the largest ratio $\langle r(h)\rangle / \delta r(h)$ of about 1.7–2. In this altitude range the aerosol is formed from particles with practically the same size $\langle r(h)\rangle \sim 0.47$ μm and $\delta r(h) \sim 0.2$. The aerosol extinction coefficient is slightly stratified (Fig. 2*a*), however the vertical profile of the ratio $\langle r(h)\rangle / \delta r(h)$ indicates the presence of four aerosol layers of up to 2 km thickness. Thus, in the 23–34 km altitude range we observed the layers of quasihomogeneous formations, whose homogeneity strengthened with decreasing altitude and reached its maximum $K_r = 2.3$ at the altitude 23.5 km. In the experiment II the altitude profile of K_r, constructed for the 23–34 km altitude range, clearly demonstrates three layers 2 km thick. These layers have microphysical characteristics similar to those obtained in experiment I(Fig. 3*c*). However, in this case the maximum $K_r = 1.8$ is reached at the altitude 28.5 km. The vertical profiles of $\langle r(h)\rangle$, $\delta r(h)$, and $\langle r(h)\rangle / \delta r(h)$ corresponding to experiment III show that in that case aerosol was the ensemble of particles with the size varying significantly: $\langle r(h)\rangle \sim 0.5$ μm with $\delta r(h) \sim 0.35$ μm at altitudes 14 – 20 km and $\langle r(h)\rangle \sim 0.3$ μm with $\delta r(h) \sim 0.2$ μm at altitudes 25 – 28 km. The vertical distribution of the extinction coefficient is stratified in the 14–20 km altitude range.

– In experiment III the sight line of the device was not normal to the horizon, that allowed the step of altitude discretization to be as short as 18 m. This, in turn, provided a possibility to refine our knowledge about the fine structure of aerosol in the stratosphere. Thus, for example, at altitudes from 15 to 21 km the aerosol is the set of “thin” layers with less than 1 km thickness (Fig. 3).

– The measurement results obtained in the experiment IV show that during the measurements the aerosol was the ensemble of particles distributed over height as 2 km – thick layers (the extinction coefficient). The mean radius of aerosol particles $\langle r(h)\rangle$ reaches its maximum ~0.8 μm at the altitudes 44 and 31 km. In the 20-45 km altitude range $\langle r(h)\rangle$ takes the values about 0.55 μm and decreases down to 0.45 μm at 15 km altitude. The value of δr throughout the entire altitude range 15–45 km is 0.3–0.35 μm. In the contour map, the aerosol region can be separated out at the altitude 30–34 km, which possesses two distribution modes: at 0.3 and 1.0 μm. This peculiarity – the bimodal distribution of aerosol – was supported when constructing the contour map of the aerosol volume distribution.

– In experiments I, III, and IV, the values of $\langle r(h)\rangle$ and $\delta r(h)$ obtained at the 20 km altitude are twice as large as the corresponding values obtained in the SAGE-II experiment.[2] The values of the mean radius $\langle r(h)\rangle$ and the rms deviation $\delta r(h)$ obtained in experiment II at altitudes 25 and 35–40 km agree well with those obtained in the SAGE-II experiment.

– In experiment II the thicknesses of the aerosol and ozone layers were 3 km at the same altitude of 25 km.

– The maps of the $\log(g(r, h))$ distribution show that along all directions aerosol mainly had the unimodal size distribution with the only exception at 30–34 km altitude range in the experiment IV.

– The ozone concentration profiles reconstructed from experiments I–III have well pronounced maxima with the values of $4.5 \cdot 10^{18}$ m^{-3} at the altitudes of 24 km (experiments I and II) and 27 km (experiment III). The profiles obtained in the experiments I and II have 5 km – wide maxima (FWHM), in the experiment III the width of the layer was about 12 km. The measurements in the experiment IV were conducted on May 31, therefore the reconstructed profile manifests the peculiarities of both May monthly average profile (curve *2*) and the June one (curve *3*), i.e., it has two maxima: the first at 24 km altitude and the second at 13 km altitude. The values of the reconstructed profiles of the ozone concentration are close to the values of the model profiles.[17,18]

CONCLUSION

Thus, the use of a multichannel spectrophotometer allows the reconstruction of the vertical profiles of the aerosol extinction coefficient $\beta^a(h)$, and the ozone concentration $N_o(h)$ to be made from the data of the atmospheric sensing from space in the 0.45–0.83 μm spectral range. In addition, the assumptions made on the aerosol type and on the profile of the aerosol refractive index allowed us to calculate for every altitude level (i.e., in 60–70 m intervals at the horizon) the particle size distribution function $g(r, h)$, as well as to estimate additionally the mean radius of aerosol particles $\langle r(h)\rangle$ and the width of the aerosol particle size distribution function $\delta r(h)$. The analysis of the vertical profiles of $\langle r(h)\rangle$ and $\delta r(h)$, with the use of the contour maps of $\log(g(r, h))$, enables us to separate out the regions where aerosol has several modes of size distribution as well as the regions of quasihomogeneous aerosol.

The reconstructed profiles of the ozone concentration, the aerosol extinction coefficient, and the effective microphysical characteristics can be used to study the dynamic processes in the stratosphere as well as the interaction between different atmospheric components.

REFERENCES

1. P.-Y. Wang and M.P. McCormick, J. Geoph. Res. **94**, No. D6, 8435–8446 (1989).
2. J.M. Livingston and P.B. Russel, J. Geoph. Res. **94**, No. D6, 8425–8433 (1989).
3. K.Ya. Kondrat'ev, G.I. Marchuk, A.A. Buznikov, et al., *Radiation Field of the Spherical Atmosphere* (State University Press, Leningrad, 1977), 216 pp.
4. G.M. Grechko, N.Ph. Elansky, et al., "The OZAPS experiment in observing the fine structure of the ozone and aerosol distribution in the atmosphere from the SALYUT–7 orbiting station," Preprint No. 8, Institute of Atmospheric Physics, Moscow (1990), 72 pp.
5. G.M. Grechko, A.S. Gurvich, N.F. Elanskii, et al., Dokl. Akad. Nauk SSSR **301**, No. 2, 306–309 (1988).
6. S.V. Loginov and V.V. Butov, in: *Abstracts of Papers at the European Symposium on Satellite and Remote Sensing II*, Paris, August 25–28, 1995, p. 39.
7. V.V. Butov and S.V. Loginov, Atmos. Oceanic Opt. **8**, No. 9, 732–736 (1995).
8. A.N. Tikhonov and V.Ya. Arsenin, *Methods for Solution of Ill-Posed Problems* (Nauka, Moscow, 1979), 285 pp.
9. V.F. Turchin and V.Z. Nozik, Izv. Vyssh Uchebn. Zaved., Ser. Fiz. Atmos. Okeana **5**, No. 1, 29–38 (1989).
10. R. Rizzi, R. Guzzi, and R. Legnani, Appl. Opt. **21**, No. 9, 1578–1582 (1982).
11. H.C. van de Hulst, *Light Scattering by Small Particles* (Willey, New York, 1957).
12. J. Casper, ed., *The Solar System*, Vol. 1, *The Sun* [Russian translation] (Foreign Literature Press, Moscow, 1957).
13. G.M. Grechko, A.S. Gurvich, et al., Tr. Gos. Opt. Inst. **71**, No. 205 (1989).
14. G.M. Krekov and R. F. Rakhimov, *Optical Lidar Model of Continental Aerosol* (Nauka, Novosibirsk, 1982), 200 pp.
15. M.S. Belen'kii, G.O. Zadde, et al., *Optical Model of the Atmosphere* (Tomsk Affiliate of the Siberian Branch of the Academy of Sciences of USSR, Tomsk, 1987), 148 pp.
16. Mc Clatchey, et al., "*A preliminary cloudless standard atmosphere for radiation computation,*" Final draft (aerosol models), International Association for Meteorology and Atmospheric Physics, Boulder, Colorado (1982), pp. 78–102.
17. G.M. Keating and D.F. Young, in: *Handbook for MAP*, University of Illinois (1985), Vol. 16, pp. 205–230.
18. J.J. Barnet and M. Corney, in: *Handbook for MAP*, University of Illinois (1985), Vol. 16, pp. 47–85.